

IntechOpen

Mobile and Wireless Communications

Physical Layer Development and Implementation

Edited by Salma Ait Fares



Sequential Blind Beamforming for Wireless Multipath Communications in Confined Areas

Salma Ait Fares¹, Tayeb Denidni², Sofiene Affes² and Charles Despins^{2,3}

¹*Tohoku University, Japan*

²*INRS-EMT, Canada*

³*Prompt-Quebec, Canada*

1. Introduction

The main cause of degradation of communication quality in harsh confined environments, such as underground mines, is multipath fading as it is typically more severe than co-channel interference (CCI) (Nerguizian et al., 2005; Chao & Chung, 1994). Usually underground communication systems are based on IEEE 802.11 standard using carrier sense multiple access with collision avoidance (CSMA-CA) that minimizes the CCI problem and leaves multipath fading as the main source of errors. This multipath phenomenon arises when a transmitted signal undergoes reflection from various obstacles in the propagation environment. This gives rise to multiple waves arriving at the receiver from different directions with different amplitudes, phases and time delays, which inflicts inter-symbol interference (ISI) and intra-symbol interference (isi) on the received signal and consequently time dispersion and fading (Saunders, 1999; Amca et al., 1999). To provide a remedy, adaptive equalizers (Amca et al., 1999), error-correcting codes (Sanada & Wang, 1997), diversity (Cozzo & Hughes, 2003), RAKE receivers for code division multiple access (CDMA) (Tanaka, 1994; Affes & Mermelstein, 2003), Coded Orthogonal Frequency Division Multiplexing (Stott, 2000), and adaptive antenna arrays (AAA) (McNeil et al., 2001; Bellofiore,a, 2002; Bellofiore,b, 2002) have been proposed. Among these, AAA techniques exploit spatial diversity by using multiple antennas. They have the potential of achieving high data-rates and increasing the capacity of mobile services by effectively reducing the multipath effect and CCI.

Adaptive antenna beamforming has been shown to be an effective mean for combating CCI and multipath propagation. Recently many different types of antenna beamforming have been developed (Lee & Choi, 2005; Youna & Un, 1994), and their design employs some information about the desired signal such as using a training sequence. Their use not only reduces the capacity of the system but also requires synchronization between the incident desired signal and the reference (sequence) one. Therefore, there is a strong demand for blind algorithms. For instance, the constant modulus algorithm (CMA) (Godara, 1997), applied in a blind AAA, is considered as a promising method in mobile communications for mitigating multipath fading and suppressing CCI signals. Unlike the least-mean-square (LMS) algorithm (Widrow, 1967), CMA-AAA does not need synchronization between the

incident desired signal and the reference signal. It improves the received signal by suppressing not only the CCI, but also the delayed paths of the desired signal (Godara, 1997). However, suppressing the multipath rays of the desired signal wastes a part of the available power and requires additional degrees of freedom, i.e., more array elements. In addition, since these arriving paths are delayed replicas of an identical source, it is desirable to separate and combine the delayed paths instead of suppressing them for received power maximization.

Several methods have been proposed to separate and combine the delayed paths. Among them, we mention the spatial domain path-diversity methods (Tanabe et al., 2000; Ogawa et al., 1999) for time division multiple access systems, based on spatial processing for efficient exploitation of the propagated energy. In these methods, multiple beams are formed to separate the direct path and the delayed paths by using training sequences. Paths with various time delay differences are separately extracted at the receiver to produce each of the multiple paths in the spatial domain. Then, the time delay difference is corrected, and the multipath signals are combined.

These aforementioned approaches have certain advantages and limitations, some of them require training sequences and all of them aim to solve the problem of ISI in multipath propagation environments, when the time path arrival (TPA) is an integer multiple of the sampling interval. Regarding the ISI problem, when the TPA is non-integer multiple of the sampling interval, other approaches are used such as Rake receiver, applied in CDMA systems, to treat the path arrivals at the chip interval (Tanaka, 1994; Affes & Mermelstein, 2003) or straightforwardly, oversampling (Amca et al., 1999; Slock, 1994) is employed. However, over-sampling will complicate the structure of the analog-to-digital converter, and also may not synchronize correctly within the actual time path arrival τ .

Generally speaking, when the TPA is a non-integer multiple of the sampling interval, the power available in these paths is wasted and the fractional time delay estimation (FTDE) is called for to overrule the over-sampling solution. FTDE filters are employed in several signal processing applications such as the estimation of the time delay difference between signals received at two spatially separated antenna arrays (So et al., 1994). They consist in using a first-order or linear interpolator to implement a Fractional Delay Filter (FDF) (So et al., 1994). An FDF is a type of digital filter designed for band-limited interpolation, which can be implemented using a Finite Impulse Response (FIR) filter based on the truncated *sinc*-interpolation method (Valimaki & Laakso, 2000).

In this Chapter, we present a new approach using sequential blind spatial-domain path-diversity beamforming (SBB) to remedy both the ISI and ISI problems using jointly CMA, LMS and adaptive FTDE filtering. This approach is designed to sequentially recover multipath rays by using multiple beamformings for received power maximization. First, the strongest path is extracted using the Modified-CMA (MCMA) (Oh & Chin, 1995; AitFares et al., 2004; AitFares et al., 2006 a; AitFares et al., 2008). Second, the paths coming with delays that are multiple integers of the sampling interval are estimated using Integer Delay-CMA SBB (ID-CMA SBB) filters adapted using LMS with the CMA delayed output as a reference signal (AitFares et al., 2004). Finally, the paths coming with fractional delays are estimated using Fractional Delay-CMA SBB (FD-CMA SBB) filters (AitFares et al., 2006 a) adapted using LMS and FTDE, the latter is implemented by an FIR *sinc*-interpolation filter (So et al., 1994). Furthermore, by relying on the common phase ambiguity characteristic presented in these extracted paths, additional enhancement is obtained by using a modified coherent

Maximum Ratio Combining (MRC) detector with hard Decision Feedback Identification (DFI) (Affes & Mermelstein, 2003; AitFares et al., 2006 b; AitFares et al., 2008) to constructively combine the different received paths for signal-to-noise ratio (SNR) maximization.

2. Modified CMA

Beamforming techniques based on blind adaptation present several comparative advantages with those based on a temporal or spatial reference. A system based on a temporal reference might carry out synchronization and demodulation, before starting weight adaptation. While a system based on a spatial reference requires strictly hardware calibration and depends on the direction of arrival information of the desired signal. On the other hand, the system based on blind adaptation does not require any information related to the antenna array geometry or the training sequences.

Many communication signals have a constant modulus (CM) property, such as, FM, PM, FSK, PSK. If these transmitted signals are affected by multipath fading, noise and/or interference, the CM property may be lost. To ease this problem, the constant modulus algorithm (CMA) has been introduced as a suitable algorithm for compensating multipath fading of constant envelope signals and has originally been proposed particularly for blind channel equalization (Godara, 1997). Afterwards, CMA has been introduced as an adaptive FIR filter for phase-modulated signals, and studied and applied to array antennas as a narrow-band adaptive beamformer to recover a constant-module signal. In fact, the CMA algorithm works with the principle that the amplitude of a signal transmitted at constant modulus and received by the array antenna, should remain constant. Hence, the main aim of an adaptive beamforming based on CMA is to restore the average of the antenna array output, $y_{CMA}(k)$, to a constant modulus as illustrated in Figure 1. That can be accomplished by adjusting the vector of beamforming weight, $w_{CMA}=[w_1, \dots, w_N]^T$, by minimizing a certain cost function. In the reference of (Godara, 1997) which uses the CMA in order to carry out blind equalization, the criterion was to minimize the function $J^{(p)}$, referred to as the dispersion of order p ($p > 0$ integer), and defined by:

$$J^{(p)}(k) = E \left[\left(|y_{CMA}(k)|^p - R_{CMA,p} \right)^2 \right], \quad (1)$$

where $E[\bullet]$ is the expectation value of $[\bullet]$, y_{CMA} is the antenna array output using CMA beamforming and R_{CMA} is a constant that depends on the transmitted symbols a and defined by

$$R_{CMA,p} = \frac{E[|a|^{2p}]}{E[|a|^p]}, \quad (2)$$

where a is the transmitted symbol. The case generally used is for $p=2$, where the cost function, $J^{(2)}$, is indeed the quadratic error between the square amplitude of the array output signal and the constant $R_{CMA,2}$, from where the equation (1) becomes

$$J^{(2)}(k) = E \left[\left(|y_{CMA}(k)|^2 - R_{CMA,2} \right)^2 \right], \quad (3)$$

where $R_{CMA,2} = \frac{E[|a|^4]}{E[|a|^2]}$. For simplicity, we denote $R_{CMA,2}$ simply as R_{CMA} .

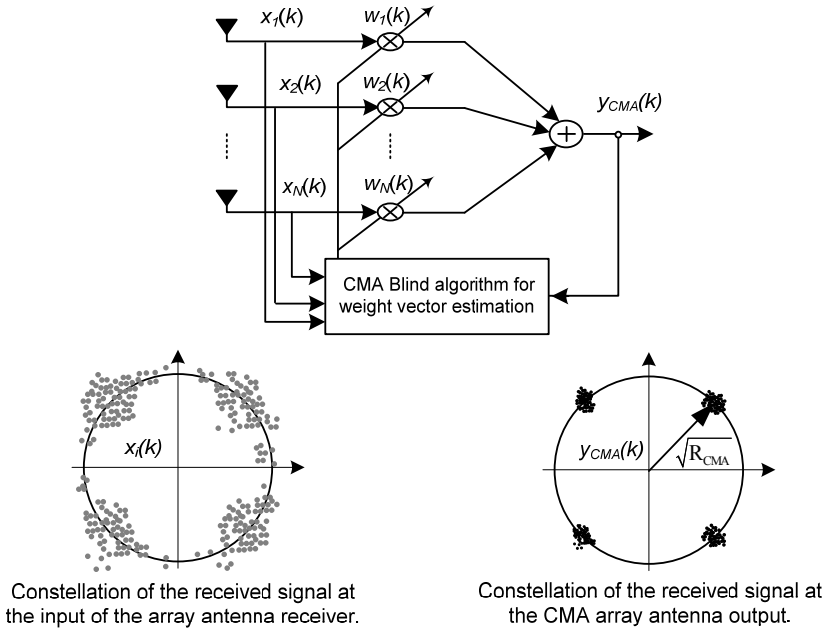


Fig. 1. Adaptive beamforming using CMA blind algorithm.

A stochastic gradient method can be used to minimize this cost function by adjusting adaptively the beamforming weight vector, w_{CMA} , according to the following expression:

$$\mathbf{w}_{CMA}(k+1) = \mathbf{w}_{CMA}(k) - \mu \cdot e^*(k) \cdot \mathbf{x}(k), \quad (4)$$

where $\mathbf{x}(k)=[x_1, \dots, x_N]^T$ represents the received signal vector and the error signal is given by

$$e(k) = y_{CMA}(k) \cdot (y_{CMA}^2(k) - R_{CMA}(k)). \quad (5)$$

The antenna array output is expressed by:

$$y_{CMA}(k) = \mathbf{w}_{CMA}^H(k) \cdot \mathbf{x}(k). \quad (6)$$

After convergence, the array output is reconstituted with a signal having a constant envelope on average, while the weight vector w_{CMA} converges to the Wiener solution.

However, from (3), since this cost function is invariable with an arbitrary phase rotation, ϕ , in the constellation of the estimated signal, i.e.

$$J_{CMA}(k) = E \left[\left(|y_{CMA}(k) \cdot e^{j\phi}|^2 - R_{CMA} \right)^2 \right] = E \left[(|y_{CMA}(k)|^2 - R_{CMA})^2 \right], \quad (7)$$

the constellation of the antenna array output may undergo an arbitrary phase rotation. In other words, the CMA algorithm restores on average the array output to a signal with a constant envelope while trying to place this output in a circle of radius $\sqrt{R_{CMA}}$ with a random phase, ϕ . Consequently, to bring back the constellation of the array output to its good position, a phase rotation mechanism is required in the CMA adaptive process. To

solve the problem of the phase rotation of the estimated signal, using CMA, without recourse to any additional phase estimation, Modified-CMA (MCMA) (Oh & Chin, 1995) is used. In the MCMA version, the cost function, given by equation (1), is divided into real and imaginary parts, so that the envelope as well as the phase will be considered in the array output estimation.

2.1 Modified – CMA algorithm

The expression of the cost function of the MCMA is expressed as follows:

$$J_{MCMA}(k) = E \left[\left(|y_{MCMA_R}(k)|^2 - R_R \right)^2 \right] + E \left[\left(|y_{MCMA_I}(k)|^2 - R_I \right)^2 \right], \quad (8)$$

where the parameters R_R and R_I are real constants defined as:

$$R_R = \frac{E[a_R^4(n)]}{E[a_R^2(n)]^2} \quad (9)$$

and

$$R_I = \frac{E[a_I^4(n)]}{E[a_I^2(n)]^2} \quad (10)$$

where

$$a_R(n) = \text{real}(a(n)), \quad (11)$$

$$a_I(n) = \text{imag}(a(n)), \quad (12)$$

where $\text{real}(\bullet)$ and $\text{imag}(\bullet)$ denote, the real and imaginary parts of (\bullet) , respectively, and $a(n)$ represents the transmitted signal sequence, $a \in A_M = \{a_1, \dots, a_M\}$, and

$$y_{MCMA_R}(k) = \text{real}(y_{MCMA}(k)), \quad (13)$$

$$y_{MCMA_I}(k) = \text{imag}(y_{MCMA}(k)). \quad (14)$$

A stochastic gradient approach can be employed in order to minimize this modified cost function, $J_{MCMA}(k)$, by adjusting adaptively the weight vector, \mathbf{w}_{MCMA} , as

$$\mathbf{w}_{MCMA}(k+1) = \mathbf{w}_{MCMA}(k) - \mu \cdot e^*(k) \cdot \mathbf{x}(k), \quad (15)$$

where μ is a small positive step size.

The error signal is expressed as:

$$e(k) = e_R(k) + j \cdot e_I(k), \quad (16)$$

where

$$e_R(k) = y_{MCMA_R}(k) \cdot (y_{MCMA_R}^2(k) - R_R), \quad (17)$$

$$e_I(k) = y_{MCMA_I}(k) \cdot (y_{MCMA_I}^2(k) - R_I). \quad (18)$$

In this case, the MCMA filter output will be expressed as:

$$y_{MCMA}(k) = \mathbf{w}_{MCMA}^H(k) \cdot \mathbf{x}(k). \quad (19)$$

In our proposed approach, we adopt the MCMA algorithm since it solves the problem of the phase rotation of the estimated signal at the array output without the need of a separate phase adaptation mechanism. The following sections propose two versions of sequential

blind beamforming (ID-CMA SBB and FD-CMA SBB), based on spatial-domain path-diversity, in order to detect, respectively, the paths arriving with multiple integer delays of the sampling interval and the paths arriving with fractional time delays, while using the MCMA beamforming output as a reference signal.

3. ID-CMA SBB Approach

For a frequency selective fading channel, we propose, in this section, a new method of path synchronization, named ID-CMA SBB (Integer Delay-CMA SBB), based on spatial-domain path-diversity (AitFares et al., 2004; AitFares et al., 2008). This approach resolves the problems involved in the presence of the ISI generated by the presence of the paths arriving with multiple integer delays of the symbol duration. However, since these delayed paths are only delayed replicas of identical sources, we may detect them while making use of the first estimated path as a reference signal. In fact, the ID-CMA approach principle consists in estimating the strongest path by using MCMA algorithm, while other auxiliary beamformers are sequentially used to extract the remaining delayed paths, arriving with integer multiple delays of the symbol duration ($k.T_s$, k is an integer).

3.1. Signal model

Consider a uniform linear array of N omni-directional antenna elements receiving L multipath signals. The received signal $x_m(k)$ at the m -th antenna can be expressed as:

$$x_m(k) = \sum_{i=1}^L \alpha_i(k) \cdot s(k - \tau_i) \cdot e^{-j\pi(m-1) \sin(D\theta A_i)} \cdot e^{-2\pi f_D k} + \eta_m(k), \quad m=1, \dots, N, \quad (20)$$

where, $\alpha_i(k)$ are the complex gains of the Rayleigh fading rays (with uniformly distributed phases φ_i between 0 and 2π) of the i -th path, $\alpha_i(k)e^{-2\pi f_D k}$ are of Jakes' model with f_D as maximum Doppler spread¹, $s(k)$ is the desired source sequence, drawn from alphabet members $A_M = \{a_1, \dots, a_M\}$, L is the number of multipath signals, τ_i is the path delay for the i -th path, $D\theta A_i$ is the direction of arrival of the i -th path and $\eta_m(k)$ is an additive white Gaussian noise process with variance σ_n^2 at the m -th receive antenna. For convenience, the array is assumed to be uniform and linear with inter-element spacing $d = \lambda/2$, where λ is the wavelength at the operating frequency.

To simplify the illustration of the proposed approach, we suppose receiving two paths ($L=2$) of which the first, of highest power, arrives at the array antenna with a time delay equal to zero, and the second with a time delay equal to T_s . Then equation (20) becomes:

$$x_m(k) = A_{1m} \cdot s(k) + A_{2m} \cdot s(k - T_s) + \eta_m(k), \quad m=1, \dots, N, \quad (21)$$

$$\text{where} \quad A_{im}(k) = \alpha_i(k) \cdot e^{-j\pi(m-1) \sin(D\theta A_i)} \cdot e^{-2\pi f_D k}, \quad m=1, \dots, N, \quad i = \{1, 2\}. \quad (22)$$

Figure 2 shows the new structure for spatial-domain path diversity to resolve multipath signals when TPAs are integer ($0, T_s$) multiples of the sampling interval. This method is implemented using two sequential beamformers. The first beamformer is used to estimate

¹ We chose here the model of a point-source propagation with no angular distribution to consider the worst-case scenario in terms of performance. However, the proposed algorithm can be applied to any channel type or angular distribution without limitation in principle.

the strongest path, and its weights (w_{MCMA}) are adapted using the MCMA. The output of this filter (y_{MCMA}) is fed into ID-CMA beamformer to construct the path arriving with an integer delay $\tau_2 = T_s$ using the LMS algorithm.

However, to ensure that the ID-CMA filter detects the path arriving with a specific integer delay, i.e. T_s , a signal canceller filter is used to extract the contribution of the already extracted path from the received signal vector. Finally, a path combination technique is used to combine these extracted paths for power maximization. This combination technique will be presented later in Section 5. In what follows, we will present the mathematical development of the shaded blocks, illustrated in Figure 2, constituting the ID-CMA SBB approach, particularly the cancellation filter of y_{MCMA} and the ID-CMA₁ filter.

By using equation (21), the MCMA filter output given by (19), becomes

$$y_{MCMA}(k) = \mathbf{w}_{MCMA}^H(k) \cdot \mathbf{A}_1(k) \cdot s(k) + \mathbf{w}_{MCMA}^H(k) \cdot \mathbf{A}_2(k) \cdot s(k - T_s) + \mathbf{w}_{MCMA}^H(k) \cdot \boldsymbol{\eta}(k), \quad (23)$$

where the vector $\mathbf{A}_i(k) = [A_{i1}(k), A_{i2}(k)]^T$ for $i=1, 2$, the element $A_{im}(k)$ is given by (22) for $m=1, 2$, and $\boldsymbol{\eta}(k) = [\eta_1(k), \dots, \eta_N(k)]^T$.

After convergence, the MCMA beamforming output can be expressed as

$$y_{MCMA}(k) \cong \hat{s}(k) + \gamma_1(k), \quad (24)$$

where the noise scalar is given by

$$\gamma_1(k) = \mathbf{w}_{MCMA}^H(k) \cdot \boldsymbol{\eta}(k), \quad (25)$$

and $\hat{s}(k)$ represents an estimation of the transmitted signal $s(k)$.

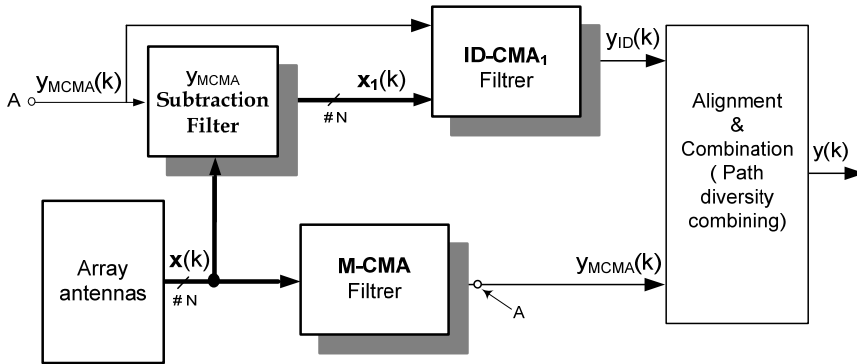


Fig. 2. The proposed ID-CMA SBB approach for extracting the direct path and delayed path arriving with an integer multiple of the sampling period equal to T_s .

3.2. First path cancelling

In order to ensure an efficient estimation of the second path using the ID-CMA₁ filter, the contribution of the first estimated path, $y_{MCMA}(k)$, should be removed from the received signal vector $x(k)$. To perform this extraction, a replica of the first detected path should be estimated, i.e., an estimate of the first path power and, then, it will be removed from the received signal vector $x(k)$. However, in what follows, we will study two techniques of

cancellation of the signal contribution by employing the method of *correlation* (Yuan & Tsai, 2005) as depicted in Figure 3(a), or by using the *Adaptive Signal Canceller* (ASC) which is particularly applied in echo cancellation processing, as illustrated in Figure 3(b) (Furukawa, 1996).

A - Correlation coefficient approach

The purpose of this method consists in calculating the correlation coefficient at each antenna element between the received signal at the m -th antenna element $x_m(k)$ and the estimated signal $y_{MCMA}(k)$, which is regarded as a reference signal. This coefficient, provided by (26), represents the quotient of the correlation between the received signal at the m -th antenna element, and the estimated signal by the MCMA filter, and the autocorrelation of this estimated signal:

$$\rho_m = \frac{E[x_m(k) \cdot y_{MCMA}^*(k)]}{E[|y_{MCMA}(k)|^2]}, \quad \text{for } m = 1, \dots, N. \quad (26)$$

By using (21), (24) and (25), and assuming all signals are decorrelated, this correlation coefficient may be simplified as

$$\begin{aligned} \rho_m &= \frac{E \left[\left(A_{1m}(k)s(k) + A_{2m}(k)s(k - T_s) + \eta_m(k) \right) \cdot \left(\hat{s}(k) + \sum_{m=1}^N w_{MCMA,m}^*(k) \cdot \eta_m(k) \right)^* \right]}{E \left[\left| \hat{s}(k) + \sum_{m=1}^N w_{MCMA,m}^*(k) \cdot \eta_m(k) \right|^2 \right]} \\ &= \frac{E[A_{1m}(k)s(k)s^*(k)]}{E[|\hat{s}(k)|^2] + E \left[\left| \sum_{m=1}^N w_{MCMA,m}^*(k) \eta_m(k) \right|^2 \right]} + \frac{E[\eta_m(k) \cdot \sum_{m=1}^N w_{MCMA,m}^*(k) \cdot \eta_m^*(k)]}{E[|\hat{s}(k)|^2] + E \left[\left| \sum_{m=1}^N w_{MCMA,m}^*(k) \eta_m(k) \right|^2 \right]}. \end{aligned} \quad (27)$$

By computing the instantaneous value for the numerator and the denominator of (27) and, by assuming that the variance of $s(k)$ is equal to one and by neglecting the terms associated to the noise power, equation (27) can be approximated by:

$$\rho_m \cong A_{1m}(k). \quad (28)$$

The signal replica $z_m(k)$ of the first path estimated at the m -th antenna element is then generated by multiplying $\rho_m(k)$ by $y_{MCMA}(k)$ as follows:

$$\begin{aligned} z_m(k) &= \rho_m(k) \cdot y_{MCMA}(k) \\ &= A_{1m}(k) \cdot \hat{s}(k) + A_{1m}(k) \cdot \gamma_1(k), \end{aligned} \quad (29)$$

where γ_1 is expressed by (25).

The second term on the right side of (29) is sufficiently small compared to the first term. Then, the signal received at the m -th antenna element, $x_{1m}(k)$, after extraction of the replica $z_m(k)$ from the received signal, $x_m(k)$, given by equation (21), will be expressed by:

$$\begin{aligned} x_{1m}(k) &= x_m(k) - z_m(k) \\ &= A_{2m}(k) \cdot s(k - T_s) + \eta_m(k), \quad m = 1, \dots, N. \end{aligned} \quad (30)$$

Even if the resulting value of the signal vector $x_1(k) = [x_{11}, \dots, x_{1N}]^T$ has a noise term, its main component contains information about the desired signal, representing the second delayed path.

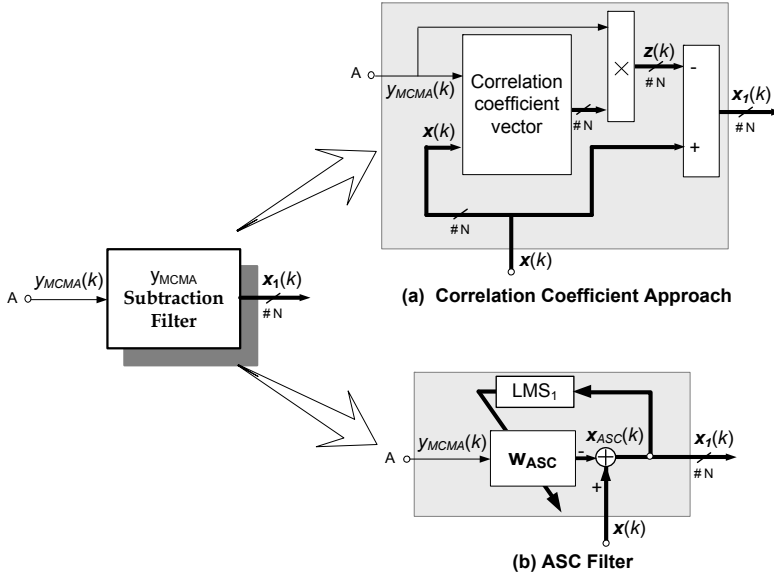


Fig. 3. Canceller Filter for the y_{MCMA} path using (a) the correlation method (b) ASC filter.

B - Adaptive Signal Canceller (ASC) approach

An alternative to remove the contribution of the first estimated path is to adjust, adaptively, the generation of the replica of the signal $y_{MCMA}(k)$, i.e., $z_m(k)$, expressed by equation (29) using the ASC filter. This real time adaptation consists in estimating the contribution of the signal related to the first path; therefore, it will be adaptively extracted to effectively remove the first path from the received signal. The principle of operation is illustrated in Figure 3(b) where the LMS algorithm is used to adjust the weights of the ASC filter.

The signal vector at the output of the ASC filter is expressed by

$$\mathbf{x}_{ASC}(k) = \mathbf{w}_{ASC}^H(k) \cdot y_{MCMA}(k), \quad (31)$$

where $w_{ASC}(k)$ represents the weight vector of the ASC filter.

By using the vector signal $\mathbf{x}(k)$ as a reference signal for the LMS algorithm, the vector error signal, $\mathbf{x}_1(k)$, of the ASC filter is expressed by:

$$\mathbf{x}_1(k) = \mathbf{x}(k) - \mathbf{x}_{ASC}(k), \quad (32)$$

where $\mathbf{x}_{ASC}(k)$ represents the signal vector of the ASC filter output.

Furthermore, the weight vector of the filter ASC is adjusted by using the LMS algorithm as follows:

$$\mathbf{w}_{ASC}(k+1) = \mathbf{w}_{ASC}(k) + \mu_1 \cdot \mathbf{x}_1^H(k) \cdot y_{MCMA}(k), \quad (33)$$

where μ_1 is a small positive step size.

It should be mentioned that the signal subtraction can be made using different adaptive algorithms, namely RLS, SML, etc. The LMS algorithm presents an acceptable convergence and is used here to ease the mathematical development of the ASC filter. In the following

sections, we favored the use of the ASC filter in our proposed SBB owing to its adaptive nature using the LMS algorithm.

3.3. ID-CMA Filter

As explained earlier, a delayed replica of the signal $y_{MCMA}(k)$ will be used as a reference signal to estimate the second path using the ID-CMA₁ filter as shown in Figure 4. To implement this proposed scheme, we delayed the output $y_{MCMA}(k)$ by a delay equal to that of the 2nd path, which is assumed here equal to T_s , (according to (21)), and then fed it back to the ID-CMA₁ filter as a reference signal for the LMS algorithm. The signal output of this ID-CMA₁ filter is expressed by:

$$y_{ID}(k) = \mathbf{w}_{ID}^H(k) \cdot \mathbf{x}_1(k), \quad (34)$$

where $\mathbf{x}_1(k)$ is the ASC filter output given by (32) and $\mathbf{w}_{ID}(k)$ is the weight vector of the ID-CMA₁ filter adjusted here by using the LMS algorithm as follows

$$\mathbf{w}_{ID}(k+1) = \mathbf{w}_{ID}(k) + \mu_2 \cdot e_{ID}^*(k) \cdot \mathbf{x}_1(k), \quad (35)$$

where μ_2 represents a small positive step size. The error signal, e_{ID} , is computed by using a delayed replica of the signal $y_{MCMA}(k)$, i.e., $y_{MCMA}(k-1)$, as a reference signal for the LMS algorithm, and it is expressed by

$$e_{ID}(k) = y_{MCMA}(k-1) - y_{ID}(k), \quad (36)$$

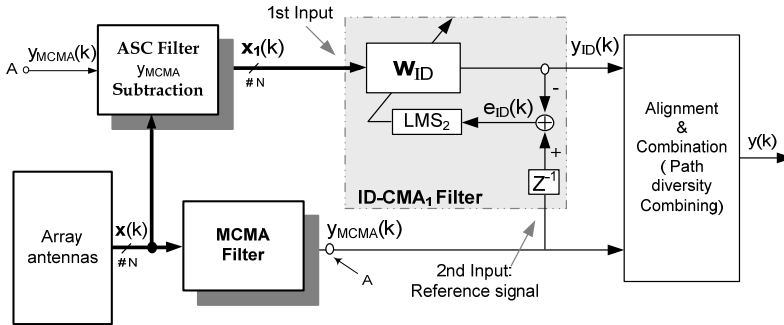


Fig. 4. ID-CMA Filter to estimation the second path arriving with delay equal to T_s .

4. FD-CMA SBB Approach

In addition to the presence of paths arriving with delays that are integer multiples of the sampling interval, some reflections in multipath propagation can arrive at the receiver between one period of two successive symbols, as illustrated in Figure 5. At the receiver side, these delayed signals can be combined in constructive or destructive manner. A constructive combination implies that the presence of this path diversity is exploited and, an improved performance is achieved. However, a destructive combination implies that the second delayed path is shifted by a certain phase and that its summation with the first path

degrades the quality of the received signal. This type of multipath effect, known as the intra-symbol interference (isi), can cause significant amplitude attenuation of the received signal, thus leading to reception errors of the desired signal.

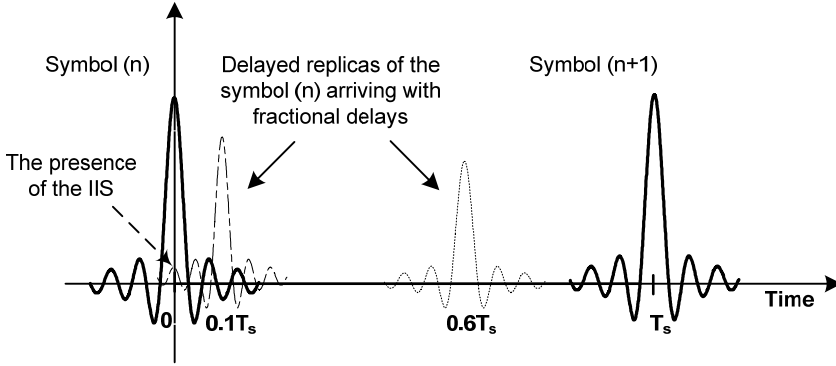


Fig. 5. Paths arrived at fractional delays.

On the other hand, at the sampling time, the information containing in this paths arriving with a delay less than the sampling interval (fractional), is generally lost and ignored by the receiver, thus leading to a reduction in the received signal power.

However, in order to maximize the received signal power, the presence of different paths, arriving with a fractional delay, may be exploited by detecting and combining them constructively. Indeed, some research works have proposed the spatio-temporal diversity techniques by using Rake receiver, applied to the CDMA system, to detect paths arriving at chip duration (Tanaka, 1994; Affes & Mermelstein, 2003), and also temporal diversity approach using an over-sampling (Slock, 1994). Other studies have also proposed a variable sampling frequency, $1/(T_s - \xi)$ where $0 \leq \xi < T_s$, to maximize the chance of detecting the path arriving with a fractional delay (Amca et al., 1999).

In what follows, we propose a space domain path-diversity technique, called FD-CMA SBB (Fractional Delay-CMA SBB), to detect the path arriving with a fractional delay, without recourse to an over-sampling neither a spatio-temporal processing or a specific application system (i.e., CDMA, TDMA). Indeed, this proposed approach is based on sequential blind CMA and nested LMS beamformings with adaptive fractional-time-delay estimation (FTDE) filter.

4.1. Signal model

To simplify the illustration of the proposed FD-CMA method, we suppose receiving two paths ($L=2$) where the first with highest power, arrives at the antenna arrays with a delay equal to zero, and second path arrives with a delay equal to $\tau < T_s$. So according to (20), the received signal at the m -th antenna element can be expressed as:

$$x_m(k) = A_{1m}s(k) + A_{2m}s(k - \tau) + \eta_m(k). \quad (37)$$

The FD-CMA SBB approach (AitFares et al., 2006 a) is illustrated in Figure 6 for this studied example. This approach consists first to estimate the first arriving path, $y_{MCMA}(k)$, using the

MCMA algorithm. The contribution of this estimate signal is removed from the received signal vector $\mathbf{x}(k)$ by using the ASC filter. Then, using this estimated $y_{MCMA}(k)$, the fractional delay and its corresponding path are detected by the FD-CMA filter. Finally, a path combining stage is used to maximize the received power. In following, the mathematical development of the FD-CMA SBB filter is presented.

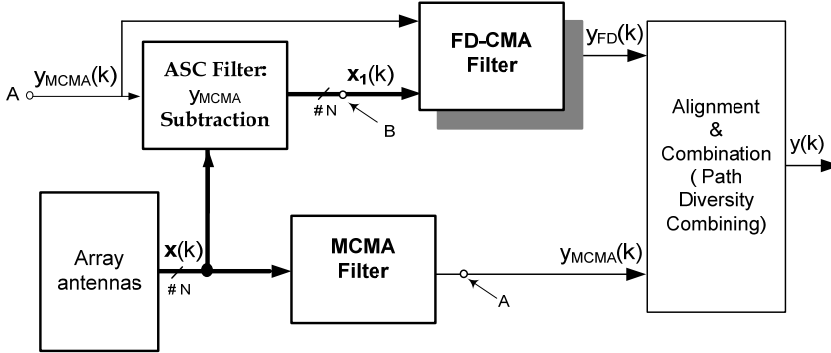


Fig. 6. The proposed FD-CMA approach to detect a path arriving with a fractional time delay and its corresponding.

4.2. FD-CMA filter

As mentioned above, the estimated signal $y_{MCMA}(k)$ will be exploited to detect the second path by using the FD-CMA filter as shown in Figure 6. After removing the contribution of the y_{MCMA} signal by the ASC filter, the signals, collected at points A and B in Figure 6, can be expressed by:

$$\text{Point A:} \quad y_{MCMA}(k) \cong \hat{s}(k) + \gamma_1(k), \quad (38)$$

$$\text{Point B:} \quad \mathbf{x}_1(k) \cong \boldsymbol{\beta}(k) \cdot s(k - \tau) + \boldsymbol{\gamma}_2(k), \quad (39)$$

where $\hat{s}(k)$ is an estimation of the transmitted symbol $s(k)$, $\boldsymbol{\beta}(k)$ is a multiplicative factor vector representing the impulse response vector of the path arriving with the fractional delay τ , and $\gamma_1(k)$ and $\boldsymbol{\gamma}_2(k)$ are additive white Gaussian noises.

By summing the vector $\mathbf{x}_1(k)$ at point B, the signal collected at point C, shown in Figure 7(a) can be expressed by:

$$\text{Point C:} \quad y_{e1}(k) = \sum_{m=1}^N \mathbf{x}_{1_m}(k) \cong \boldsymbol{\beta}(k) \cdot s(k - \tau) + \gamma(k), \quad (40)$$

where $\boldsymbol{\beta}(k) = \sum_{m=1}^N \boldsymbol{\beta}_m(k)$, $\gamma(k) = \sum_{m=1}^N \gamma_{2_m}(k)$ and the notation $\mathbf{v}_m(k)$ denotes the m -th element of the vector $\mathbf{v}(k)$.

Therefore, the signals received at points A and C, illustrated in Figure 7(a) can be regarded as two signals received by two spatially separated virtual antenna array elements, where the time delay τ represents the fractional time delay propagation between these two virtual antenna array elements, as shown in Figure 7(b), and the parameter D represents the time delay propagation between two antennas.

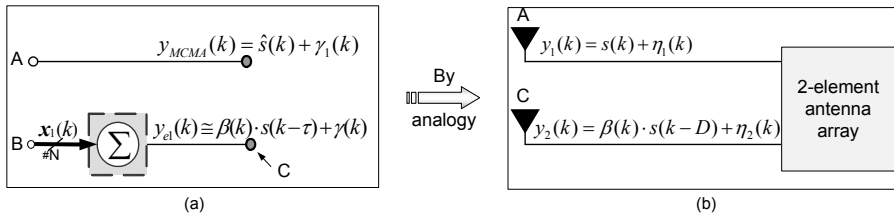


Fig. 7. By adding the elements of the vector signal at point B, the two signals capted at points A and C are seen as two signals received by a virtual 2-element antenna array.

Consequently, by analogy with the fractional delay filter (FDF) proposed in (So et al., 1994), the fractional time delay between the signals $s(k)$ and $s(k-\tau)$ can be estimated using the fractional time delay estimation filter (FTDE) proposed in (So et al., 1994). This FTDE filter consists of a linear interpolator which can be implemented using an FIR filter based on the truncated *sinc*-interpolation method. In fact, this FIR filter in (So et al., 1994) is designed to estimate the fractional time delay D by minimizing the square error, $|e_n(k)|^2$, where the signal received by the 2nd antenna is taken as a reference signal for the LMS algorithm as shown in Figure 8.

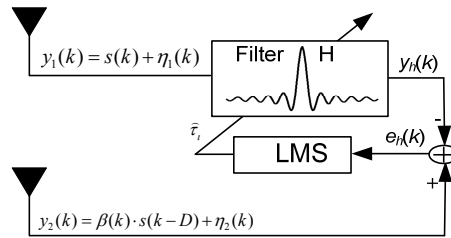


Fig. 8. FTDE filter used to estimate the fractional time delay propagation (D) between two spatially separated antennas.

We have developed this FTDE filter for complex signals, and subsequently we have adopted it in our work, to estimate the fractional time delay of the second path, as shown in Figure 9. However, instead of summing directly the signal $x_1(k)$ at point B (as shown in Figure 9) to construct the reference signal of the FTDE filter, the beamforming filter w_{FD} , is inserted at point B to construct the FD-CMA filter and estimate the fractional time delay and its corresponding path as depicted in Figure 10. The weight vector of this filter (w_{FD}) is adapted using LMS algorithm (LMS₅ in Figure 10), where the first beamformer output, y_{MCMA} , is fed into the FTDE filter to generate a reference signal for the LMS algorithm, i.e., $y_{MCMA}(k - \hat{\tau})$. The weight adaptation for both FTDE and w_{FD} filters is nested in the sense that the output of the w_{FD} beamforming filter is used as a reference signal for FTDE filter and vice-versa. The delay block is inserted in order to align temporally the two signals and y_h and $x_{1,D}$, that we will explain later.

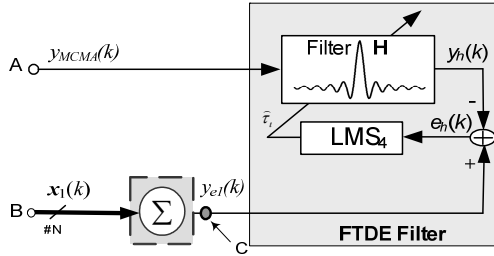


Fig. 9. FTDE filter for estimating the fractional delay of the signal received at point C.

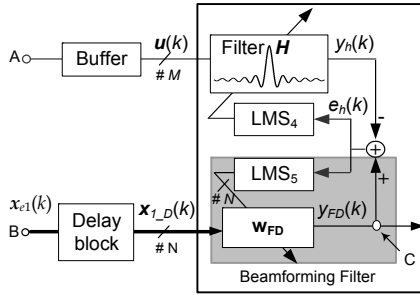


Fig. 10. FD-CMA Filter for fractional time delay estimation and its corresponding path detection.

The following subsections present the FTDE filter developed and adopted in this work, and adaptive beamforming to estimate, the fractional delay and its corresponding path, respectively.

A- Fractional Time Delay Estimation

Once the first path is estimated by the MCMA filter, it is delayed by an estimated value $\hat{\tau}$ using the fractional time delay filter H . This filtering is carried out by using the following equation using ideal fractional-delay filter with *sinc* function interpolation:

$$\begin{aligned} y_h(k) &\cong y_{MCMA}(k - \hat{\tau}) \\ &= \sum_{n=-\infty}^{\infty} \text{sinc}(n - \hat{\tau}) \cdot y_{MCMA}(k - n) \\ &= \sum_{n=-P}^P \text{sinc}(n - \hat{\tau}) \cdot y_{MCMA}(k - n), \end{aligned} \quad (41)$$

where the infinity sign in the summation is replaced by an integer P , which is chosen sufficiently large to minimize the truncation error. $\hat{\tau}$ is the instantaneous estimated time delay. If $\hat{\tau}$ is a fractional number, i.e. $0 < \hat{\tau} < 1$, the *sinc* interpolation impulse response has non-zero values for all n :

$$0 < \tau < 1 \rightarrow \text{sinc}(n - \tau) \neq 0, \quad \forall n \in \mathbb{Z}. \quad (42)$$

The delayed signal, $y_h(k)$, is the output of the FIR filter H whose coefficients are $\text{sinc}(n - \hat{\tau})$ and input is $y_{MCMA}(k)$. For this issue, a lookup table of the *sinc* function is constructed that consists of a matrix H of dimension $K \times (2P+1)$, with a generic element:

$$h_{ij} = \text{sinc}\left(\frac{i-1}{K} - j\right), \quad 1 \leq i \leq K, -P \leq j \leq P, \quad (43)$$

where K represents the inverse resolution over T_s of the estimated delay $\hat{\tau}$. The theoretical elements of the i -th row of the matrix \mathbf{H} are therefore identical to the samples of the truncated *sinc* function with delay equal to:

$$\tau_i = \left(\frac{i-1}{K}\right), \quad 1 \leq i \leq K. \quad (44)$$

For the time delay estimation process, only the estimated time delay $\hat{\tau}_i(k)$ is adapted in our approach, and it is used as an index to obtain the vector \mathbf{h}_i from a lookup table. As mentioned previously, this lookup table is a two-dimensional matrix called \mathbf{H} of size $K \times (2P+1)$ that contains samples of the *sinc* function with delay ranging from 0 to $(K-1)/K$. For a given vector τ with theoretically delayed value elements τ_i given by (44), the i -th row is computed as follows

$$i = \tau_i \cdot K + 1. \quad (45)$$

So, at each iteration, the integer part of $(\tau_i \cdot K + 1)$ is used to locate the i -th row of the matrix \mathbf{H} , i.e. \mathbf{h}_i , that is used to delay the signal $y_{MCMA}(k)$ using

$$y_h(k) = \mathbf{h}_i^H \cdot \mathbf{u}(k), \quad (46)$$

where $\mathbf{u}(k)$ is given by:

$$\mathbf{u}(k) = [y_{MCMA}(k), \dots, y_{MCMA}(k - (2P + 1))]^T. \quad (47)$$

The estimated fractional time delay is obtained by using the gradient descent of the instantaneous squared error $|e_h|^2$ surface to locate the global minimum, i.e., using LMS (So et al., 1994). The estimated gradient is equal to the derivative of $|e_h|^2$ with respect to $\hat{\tau}$. The FTDE algorithm may be summarized as follows. The complex error signal, $e_h(k)$, is given by:

$$\begin{aligned} e_h(k) &= y_{FD}(k) - y_h(k) \\ &= y_{FD}(k) - \sum_{n=-P}^P \text{sinc}(n - \hat{\tau}) \cdot y_{MCMA}(k - n), \end{aligned} \quad (48)$$

where

$$y_{FD}(k) = \mathbf{w}_{FD}^H(k) \cdot \mathbf{x}_{1,D}(k), \quad (49)$$

$$\mathbf{x}_{1,D}(k) = \mathbf{x}_1(k - (P + 1)). \quad (50)$$

$\mathbf{x}_{1,D}(k)$ is delayed by $(P + 1) \cdot T_s$ to be aligned with the output of the filter \mathbf{H} , i.e., $y_h(k)$, that has latency depending on its order value $M = 2P + 1$ as shown in Figure 10. The estimated time delay can be adapted by minimizing the cost function given by:

$$J(\tau, \mathbf{w}_{FD}) = E[|e_h(k)|^2] = E[|y_{FD}(k) - y_h(k)|^2]. \quad (51)$$

The constrained LMS algorithm becomes:

$$\hat{\tau}(k + 1) = \hat{\tau}(k) - \mu_4 \cdot \nabla J(\tau, \mathbf{w}_{FD}), \quad (52)$$

where μ_4 is a small positive step size.

By differentiating the instantaneous error surface, $|e_h(k)|^2$, with respect to the estimated time delay, we have:

$$\begin{aligned}
\frac{\partial(e_h^2(k))}{\partial\hat{\tau}(k)} &= \frac{\partial e_h(k)}{\partial\hat{\tau}(k)} \cdot e_h^*(k) + \frac{\partial e_h^*(k)}{\partial\hat{\tau}(k)} \cdot e_h(k) \\
&= \sum_{n=-P}^P \frac{-\partial(\text{sinc}(n-\hat{\tau}))}{\partial\hat{\tau}(k)} y_{MCMA}(k-n) e_h^*(k) - \sum_{n=-P}^P \frac{\partial(\text{sinc}(n-\hat{\tau}))}{\partial\hat{\tau}(k)} y_{MCMA}^*(k-n) e_h(k) \\
&= \sum_{n=-P}^P f(n-\hat{\tau}) y_{MCMA}(k-n) e_h^*(k) + \sum_{n=-P}^P f(n-\hat{\tau}) y_{MCMA}^*(k-n) e_h(k), \quad (53)
\end{aligned}$$

where
$$f(v) = \frac{\cos(\pi v) - \text{sinc}(v)}{v}. \quad (54)$$

Finally, the estimated time delay $\hat{\tau}$ is given by:

$$\begin{aligned}
\hat{\tau}(k+1) &= \hat{\tau}(k) - \mu_4 \cdot [\sum_{n=-P}^P f(n-\hat{\tau}) \cdot y_{MCMA}(k-n) \cdot e_h^*(k) \\
&\quad + \sum_{n=-P}^P f(n-\hat{\tau}) \cdot y_{MCMA}^*(k-n) \cdot e_h(k)]. \quad (55)
\end{aligned}$$

In our implementation, lookup tables of \cos and sinc functions are constructed for different values of v and used to calculate $f(n-\hat{\tau}(k))$. At each iteration, the integer part of $(\hat{\tau}_i(k) \cdot K + 1)$ is used to locate the i -th row of the matrix H , i.e. \mathbf{h}_i that is used to delay the signal $y_{MCMA}(k)$ by the estimated fractional delay $\hat{\tau}$ using (46).

B- Beamforming for fractional-delay path extraction

Now to extract the fractional-delay path, the weight vector of the FD-CMA filter is adapted using LMS by minimizing the cost function given in (51) as follows:

$$\mathbf{w}_{FD}(k+1) = \mathbf{w}_{FD}(k) + \mu_5 \cdot e_h^*(k) \cdot \mathbf{x}_{1,D}(k), \quad (56)$$

where μ_5 is a small positive step size.

5. General SBB Approach

According to statistical modeling presented in (Boutin et al., 2008) of the studied underground channel, we were able to characterize, among many other channel parameters, the maximum number of paths at a given operation frequency and a given path resolution. Thus, we can assume for a given transmission rate and modulation type that the maximum number of paths arriving with delays that are a multiple integer of the sampling interval as well as the maximum number of paths arriving with fractional time delays are both predicted accurately. Consequently, we assume n paths causing ISI and p paths causing isi. In this general case of the presence of paths arriving with integer and fractional delay multiples of the sampling intervals, the two ID-CMA SBB and FD-CMA SBB proposed methods can be combined in a single approach named here as General Sequential Blind Beamforming (G-SBB) approach.

To simplify, the following study is performed using a three-path channel model for illustration purposes where the TPAs are given by $\tau_1 = 0$ (the strongest path), $\tau_2 = \tau < T_s$, and $\tau_3 = T_s$. Hence the received signal at the m -th antenna can be expressed by:

$$x_m(k) = A_{1m}s(k) + A_{2m}s(k-\tau) + A_{3m}s(k-T_s) + \eta_m(k). \quad (57)$$

Figure 11 depicts the new approach using sequential blind spatial-domain path-diversity beamforming (SBB) to remedy both the ISI and isi problems using jointly CMA, LMS and adaptive FTDE filtering. This approach is designed to sequentially recover multipath rays

by using multiple beamformings for received power maximization. First, the strongest path is extracted using the MCMA (AitFares et al., 2004; AitFares et al., 2006 a; AitFares et al., 2006 b; AitFares et al., 2008). Second, the path coming with delay that is multiple integer of the sampling interval is estimated using ID-CMA filter (i.e., y_{ID}) adapted using LMS with the CMA delayed output as a reference signal (AitFares et al., 2004). Finally, the path coming with fractional delay is estimated using FD-CMA filter (i.e., y_{FD}) (AitFares et al., 2006 a) adapted using LMS and FTDE. However, in order to ensure the estimated path arriving with the fractional delay, two ASC filters are used to extract the contribution of path $y_{MCMA}(k)$ and $y_{ID}(k)$ from the received signal vector $x(k)$. As for the estimated path combination, we propose in the next section a combination based on MRC.

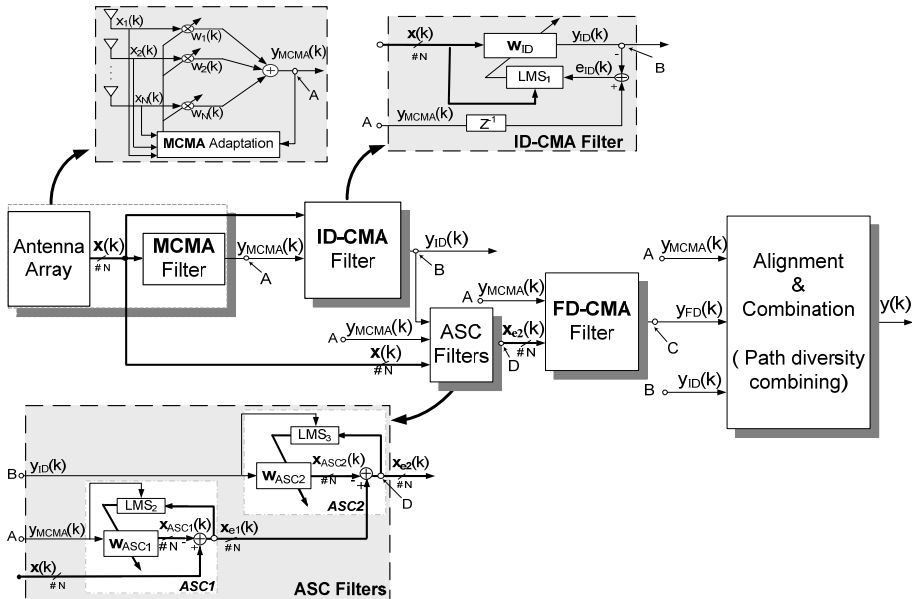


Fig. 11. Proposed G-SBB approach.

6. MRC Path Combination

The paths y_{MCMA} , y_{FD} and y_{ID} , estimated by the filters MCMA, FD-CMA and ID-CMA, respectively, possess a common phase ambiguity, since they are sequentially extracted using y_{MCMA} as a reference signal. As a result, a combination based on a simple addition of the estimated paths can only be constructive and it represents the output of a coherent Equal Gain Combiner (EGC) as illustrated in Figure 12(a). After appropriate delay alignments, the final estimated signal is given by EGC combining of the extracted paths as follows:

$$y(k) = y_{MCMA}(k) + y_{FD}(k) + y_{ID}(k + 1). \quad (58)$$

For a Differential Binary Phase Shift Keying (DBPSK) modulation scheme, where the common phase ambiguity is actually a sign ambiguity, an EGC is equivalent to MRC.

However, for higher order modulations such as Differential Quadrature Phase Shift Keying (DQPSK), where the common phase ambiguity is an unknown angular rotation, more substantial improvement compared to EGC can be obtained by implementing coherent MRC with hard DFI as shown in Figure 12(b), which strives to force this common phase ambiguity to known quantized values that keep the constellation invariant by rotation (Affes & Mermelstein, 2003), thereby allowing coherent demodulation and MRC detection. In the first step, all paths y_{MCMA} , y_{FD} and y_{ID} are aligned by appropriate additional delays, and then scaled by an MRC weighting vector $g(k)$. The summation of these scaled paths, $\tilde{s}(k)$, is given by

$$\tilde{s}(k) = \mathbf{g}^H(k) \cdot \mathbf{y}_d(k), \quad (59)$$

where
$$\mathbf{y}_d(k) = [y_{MCMA}(k), y_{FD}(k), y_{ID}(k+1)]^T, \quad (60)$$

$$\mathbf{g}(k) = [g_1(k), g_2(k), g_3(k)]^T. \quad (61)$$

In the next step, $\tilde{s}(k)$, is quantized by making a hard decision to match it to a tentative symbol $\hat{s}_h(k)$. This coherent-detection operation can be expressed as follows:

$$\hat{s}_h(k) = \text{Hard}\{\tilde{s}(k)\} = \arg_{a_k \in A_M} \min\{|\tilde{s}(k) - a_k|\}, \quad (62)$$

where A_M represents the MPSK modulation constellation defined by:

$$A_M = \{\dots, a_k, \dots\} = \left\{ \dots, e^{\frac{j\pi((2k-1)-\delta(M-2))}{M}}, \dots \right\}; \quad k \in \{1, \dots, M\}. \quad (63)$$

Since $\hat{s}_h(k)$ provides a selected estimate of the desired signal, it can be used as a feedback reference signal to update the weight vector $g(k)$ using LMS-type adaptation referred to as Decision Feedback Identification (DFI):

$$\hat{\mathbf{g}}(k+1) = \hat{\mathbf{g}}(k) - \mu_6 \cdot (\mathbf{y}_d(k) - \hat{\mathbf{g}}(k) \cdot \hat{s}_h(k)) \cdot \hat{s}_h^*(k), \quad (64)$$

where μ_6 is a small positive step size.

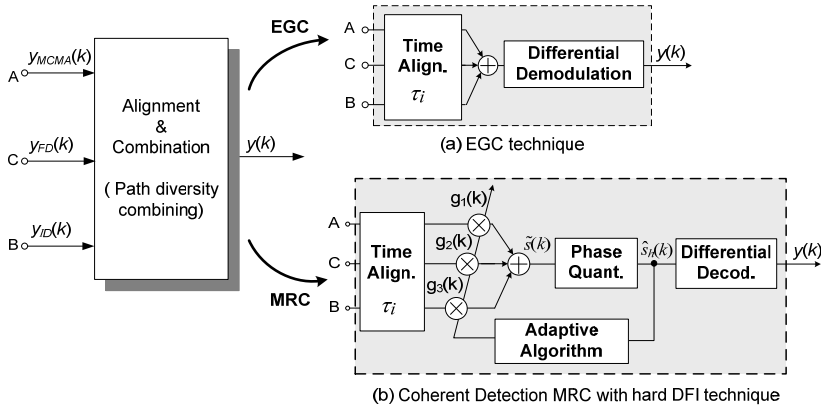


Fig. 12. Path diversity combining stage for the SBB using EGC or Coherent MRC with hard DFI.

It is this DFI procedure that enables coherent MRC detection by forcing the common phase ambiguity of the extracted paths to a value by which the constellation is invariant by rotation (Affes & Mermelstein, 2003; Aitfares et al., 2008). Finally the desired output signal $y(k)$ is estimated from $\hat{s}_h(k)$ by differential decoding, as shown in Figure 12(b), instead of differential demodulation needed previously with simple EGC. This final decoding step is expressed by:

$$y(k) = \hat{s}_h(k) \cdot s_h^*(k-1). \quad (65)$$

The proposed SBB technique enabling MRC path diversity combining (i.e., MRC-SBB) offers an SNR gain of about 2 dB gain compared to that using simple EGC implementation (i.e., EGC-SBB) (Affes & Mermelstein, 2003; Aitfares et al., 2008).

7. Computer simulation results

In this section, simulation results are presented to assess the performance of the proposed SBB method and to compare it with MCMA beamforming (Oh & Chin, 1995). A two-element array with half-wavelength spacing is considered. A desired signal is propagated along four multipaths to the antenna array while the interference and noise are simulated as additive white Gaussian noise. The first path is direct with a path arrival-time delay $\tau_1 = 0$. The second and third paths arrive, respectively, with delays τ_2 and τ_3 lower than the sampling interval, and the last path arrives with delay $\tau_4 = T_s$. Differential encoding is employed to overcome the phase ambiguity in the signal estimation. Performance study was carried out with two channel models and for two kinds of modulation (DBPSK and DQPSK). Type-A channel is Rayleigh fading with a Doppler shift $f_{d1} = 20$ Hz. Type-B channel is Rayleigh fading with a higher Doppler shift $f_{d2} = 35$ Hz. The use of these two Doppler frequencies reflects the typical range of the vehicle speed in underground environments². The Bit Error Rate (*BER*) performance for different Doppler frequencies (f_{d1} and f_{d2}) was also studied. The figure of merit is the required SNR to achieve a *BER*³ below 0.001. Table 1 summarizes the system parameters for the computer simulations.

² For operations at a carrier frequency $f_c = 2.4$ GHz and vehicle speeds $v_1 = 10$ km/h, and $v_2 = 15$ km/h, we found approximately that $f_{d1} = 20$ Hz and $f_{d2} = 35$ Hz.

³ The *BER* is calculated after steady-state convergence to avoid biasing the results.

Modulation	DBPSK or DQPSK.
Antenna array type	Linear uniform, with $\lambda/2$ element spacing.
Antenna array size	2 elements or 4 elements.
Max. Doppler frequency	$f_{d1}=20\text{Hz}$ and $f_{d2}=35\text{Hz}$.
Channel model	Type-A: Rayleigh fading with f_{d1} Type-B: Rayleigh fading with f_{d2}
Adaptive algorithm	CMA & LMS
Carrier Frequency	$f_c=2.4\text{GHz}$
Noise	AWGN
Filter order	$M=21$
Path resolution	$K=200$, i.e. $T_r=0.005 T_s$
Step sizes	$\mu=0.009$; $\mu_1=0.008$; $\mu_2=0.0095$; $\mu_3=0.008$; $\mu_4=0.001$; $\mu_5=0.009$ and $\mu_6=0.001$.
Number of symbol	10.000

Table 1. Simulation parameters.

Figs. 13 and 14 show the measured BER performance versus SNR of G-SBB and MCMA for Type-A and -B channels, with different values of τ_2 and τ_3 using a DBPSK modulated signal. As expected, it can be noted that for both algorithms, the BER performance decreases with increasing Doppler frequency values. Despite the speed increasing due to the Doppler effect, the proposed algorithm G-SBB provides significant gains and outperforms MCMA by approximately 5 dB for both channel environments (A and B).

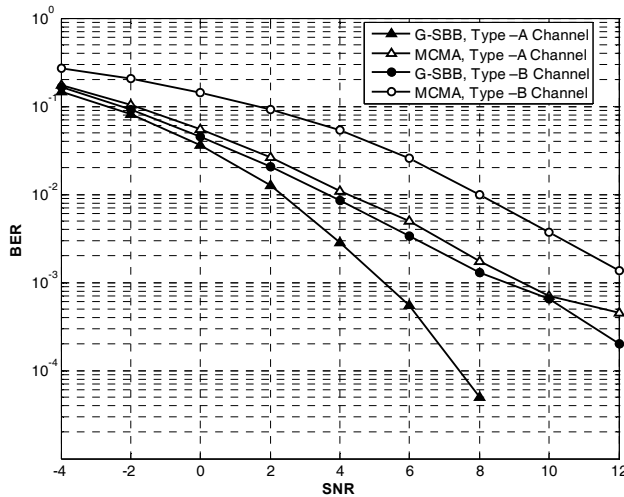


Fig. 13. BER performance versus SNR with $\tau_2=0.4T_s$ and $\tau_3=0.8T_s$ for DBPSK modulation scheme using a 2-element antenna array.

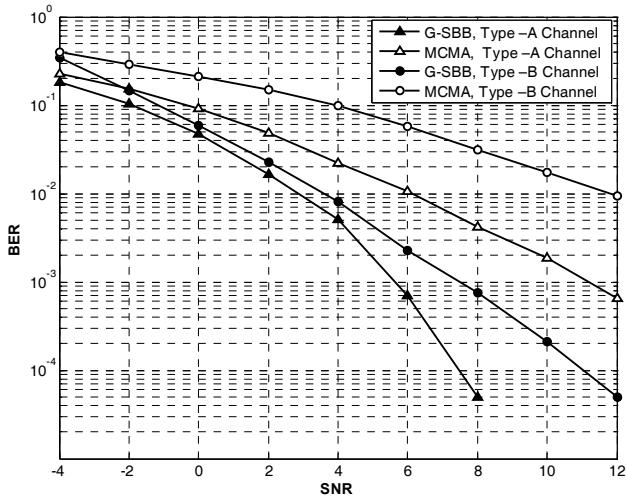


Fig. 14. BER performance versus SNR with $\tau_2=0.3T_s$ and $\tau_3=0.7T_s$ for DBPSK modulation scheme using a 2-element antenna array.

Let us now study the convergence rate of the proposed G-SBB method compared to the MCMA algorithm for the Type-A channel with $\tau_2=0.4 T_s$ and $\tau_3=0.8 T_s$ at 2.4 GHz and for SNR = 4 dB. Figure 15 illustrates the average BER in terms of the number of iterations for the first 8000 samples. A benchmark comparison with AAA using the LMS algorithm is also provided. From Figure 15, it can be seen that the LMS algorithm is the fastest one followed by the MCMA and then the G-SBB algorithms. However, the proposed G-SBB algorithm reaches a much lower steady-state BER after convergence within a shorter delay compared to AAA and MCMA.

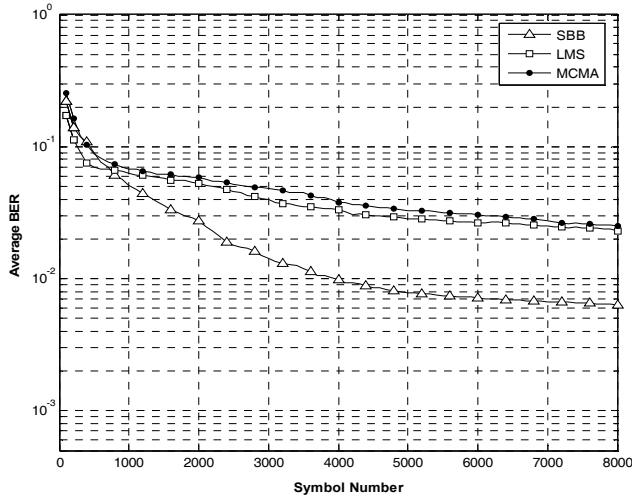


Fig. 15. The real-time performance of the proposed system compared with the MCMA and LMS algorithms at SNR = 4 dB for DBPSK modulation scheme using a 2-element antenna array.

Here we discuss the trade-off between the hardware complexity related to the delay resolution implementation and the BER performance. As mentioned above, K , given in equation (44), represents the number of the tap filter coefficients used to implement the fractional delay resolution. For instance, when $K = 10$, the delay resolution is equal to $T_r = 1/(K.T_s) = 0.1 T_s$. By increasing the value of K , we increase the FTDE resolution and consequently the FTDE filter will be able to estimate faithfully the fractional delay path which will in turn improve the BER performance. On the other hand, increasing K increases the hardware complexity needed to implement the FTDE. To find an optimal trade-off between resolution and hardware complexity, several simulations with different values of K in terms of BER performance were conducted.

Figure 16 illustrates the simulated BER performance versus SNR of the G-SBB for Type-A channel environment at different values of T_r . From this figure, it can be seen that the resolution of K impacts greatly the BER performance when K is less than 50. For K greater than 50, the optimal performance is attained and further increase of the K value is unnecessary.

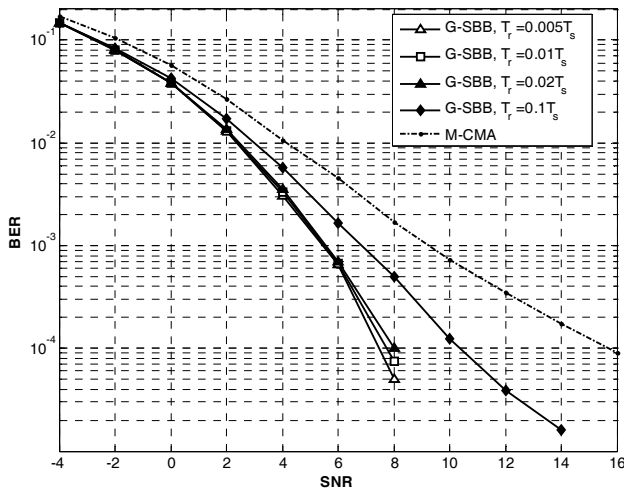


Fig. 16. BER performance versus SNR in Type -A Channel for $\tau_2 = 0.4T_s$ and $\tau_3 = 0.8T_s$ when T_r is varied using a 2-element antenna array.

For high order modulation using DQPSK, Figs. 17 and 18 illustrate the BER performance versus SNR for G-SBB using MRC or EGC in the combining step for Type-A and -B channels with $\tau_2 = 0.4 T_s$ and $\tau_3 = 0.8 T_s$, respectively, at 2.4 GHz. A benchmark comparison with AAA using MCMA is also provided. For the type-A channel, the results show that G-SBB with MRC provides a good enhancement and outperforms G-SBB with EGC and the AAA using MCMA by approximately 2 dB and up to 7 dB at a required $BER = 0.001$, respectively (Figure 17). For the type-B channel with higher Doppler frequency, the measured results show that G-SBB with MRC maintains its advantage compared to G-SBB with EGC and to the AAA using MCMA where improvements of approximately 2 dB and up to 7 dB at a required $BER = 0.001$ are obtained, respectively (Figure 18).

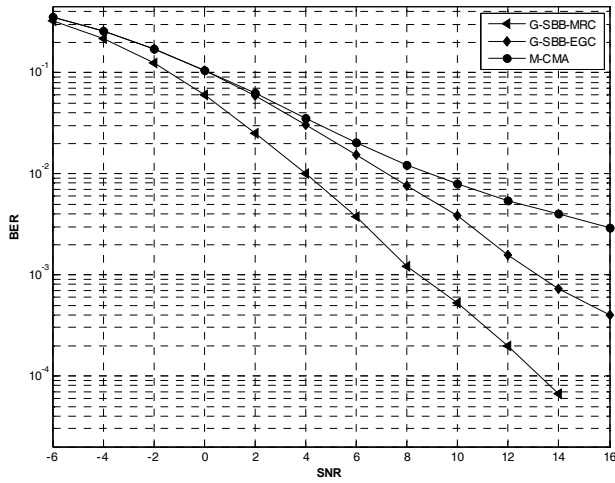


Fig. 17. BER performance versus SNR for Type -A Channel with $\tau_2=0.4T_s$ and $\tau_3=0.8T_s$ for DQPSK modulation scheme using a 2-element antenna array.

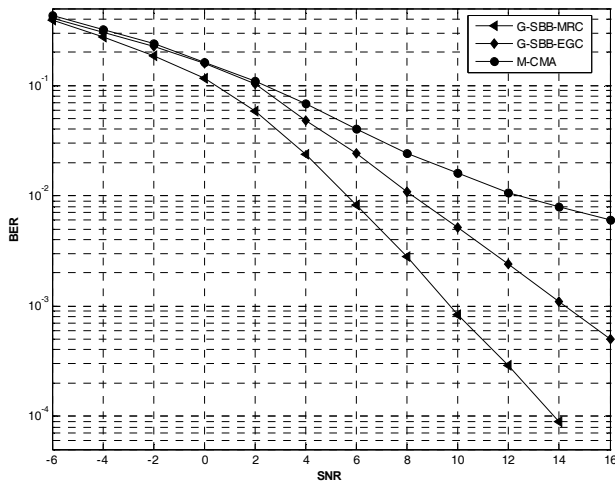


Fig. 18. BER performance versus SNR for Type -B Channel with $\tau_2=0.4T_s$ and $\tau_3=0.8T_s$ for DQPSK modulation scheme using a 2-element antenna array.

Figure 19 shows the measured BER performance versus SNR for G-SBB using MRC or EGC in the combining step and with MCMA-AAA for Type-A channel using four antenna elements ($N = 4$). Again, it is clear that the G-SBB using the proposed MRC is more efficient than both previous G-SBB versions using EGC and the conventional MCMA algorithm.

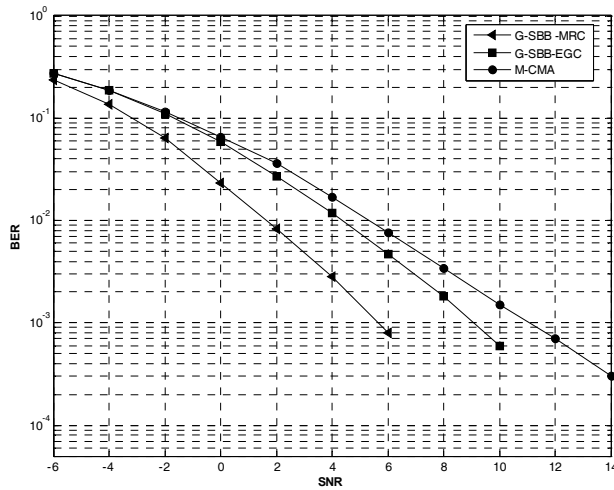


Fig. 19. BER performance versus SNR for Type -A Channel with $\tau_2=0.2T_s$ and $\tau_3=0.8T_s$ for DQPSK modulation scheme using a 4-element antenna array.

8. Conclusion

In this Chapter, a new approach using sequential blind spatial-domain path-diversity beamforming (SBB) to remedy the ISI and isi problems has been presented. Using jointly CMA, LMS and adaptive FTDE filtering, this approach has been designed to sequentially recover multipath rays to maximize the received power by extracting all dominant multipaths. MCMA is used to estimate the strongest path while the integer path delay is estimated sequentially using adapted LMS with the first beamformer output as a reference signal. A new synchronization approach for multipath propagation, based on combining a CMA-AAA and adaptive fractional time delay estimation filtering, has been proposed to estimate the fractional path delay. It should be noted that the G-SBB architecture can be generalized for an arbitrary number of received paths causing ISI where several concurrent filters (ID-CMA and FD-CMA) can be implemented to resolve the different paths. Finally, to combine these extracted paths, an enabling MRC path diversity combiner with hard DFI has also been proposed. Simulation results show the effectiveness of the proposed SBB receiver especially at high SNR, where it is expected to operate in a typical underground wireless environment (Nerguizian et al., 2005).

9. References

- AitFares, S.; Denidni, T. A. & Affes, S. (2004). Sequential blind beamforming algorithm using combined CMA/LMS for wireless underground communications, in *Proc. IEEE VTC'04*, vol. 5, pp. 3600-3604, Sept. 2004.
- AitFares, S.; Denidni, T. A.; Affes, S. & Despains, C. (2006). CMA/fractional delay sequential blind beamforming for wireless multipath communications, in *Proc. IEEE VTC'06*, vol. 6, pp. 2793-2797, May 2006.
- AitFares, S.; Denidni, T. A.; Affes, S. & Despains, C. (2006). Efficient sequential blind beamforming for wireless underground communications, in *Proc. IEEE VTC'06*, pp. 1-4, Sept. 2006.
- AitFares, S.; Denidni, T. A.; Affes, S. & Despains, C. (2008). Fractional-Delay Sequential Blind Beamforming for Wireless Multipath Communications in Confined Areas. *IEEE Transactions on Wireless Communications*, vol. 7, no. 1, pp. 1-10, January 2008.
- Affes, S. & Mermelstein, P. (2003). Adaptive space-time processing for wireless CDMA, chapter 10, pp. 283-321, in *Adaptive Signal Processing: Application to Real-World Problems*, J. Benesty and A. H. Huang, eds. Berlin: Springer, 2003.
- Amca, H.; Yenal, T. & Hacioglu, K. (1999). Adaptive equalization of frequency selective multipath fading channels based on sample selection, *Proc. IEE on Commun.*, vol. 146, no. 1, pp. 55-60, Feb. 1999.
- Bellofiore, S.; Balanis, C. A.; Foutz, J. & Spanias, A. S. (2002). Smart antenna systems for mobile communication networks, part 1: overview and antenna design, *IEEE Antennas Propag. Mag.*, vol. 44, no. 3, pp. 145-154, June 2002.
- Bellofiore, S.; Foutz, J.; Balanis, C. A. & Spanias, A. S. (2002). Smart-antenna systems for mobile communication networks, part 2: beamforming and network throughput, *IEEE Antennas Propagation Magazine*, vol. 44, no. 4, pp. 106-114, Aug. 2002.
- Boutin, M. ; Benzakour, A.; Despains, C & Affes, S. (2008). Radio Wave Characterization and Modeling in Underground Mine Tunnels, *IEEE Transaction on Antennas and Propagation*, vol. 56, no. 2, pp. 540-549, February 2008.
- Chao, R. Y. & Chung, K. S. (1994). A low profile antenna array for underground mine communication, in *Proc. ICCS 1994*, vol. 2, pp. 705-709, 1994.
- Cozzo, C. & Hughes, B. L. (2003). Space diversity in presence of discrete multipath fading channel, *IEEE Trans. Commun.*, vol. 51, no. 10, pp. 1629-1632, Oct. 2003.
- Furukawa, H.; Kamio, Y. & Sasaoka, H. (1996). Co-Channel interference reduction method using CMA adaptive array antenna, *IEEE International Symposium on Personal, Indoor and Mobile Radio Communications*, vol. 2, pp. 512-516, 1996.
- Godara, L. C. (1997). Applications of antenna arrays to mobile communications, part I: performance improvement, feasibility, and system considerations, *Proc. IEEE*, vol. 85, no. 7, pp. 1031-1060, July 1997.
- Lee, W. C. & Choi, S. (2005). Adaptive beamforming algorithm based on eigen-space method for smart antennas, *IEEE Commun. Lett.*, vol. 9, no. 10, pp. 888-890, Oct. 2005.
- McNeil, D.; Denidni, A. T. & Delisle, G. Y. (2001). Output power maximization algorithm performance of dual-antenna for personal communication handset applications, in *Proc. IEEE Antennas and Propagation Society International Symposium*, vol. 1, pp. 128-131, July 2001.

- Nerguizian, C.; Despins, C; Affes, S. & Djadel, M. (2005). Radio-channel characterization of an underground mine at 2.4 GHz wireless communications, *IEEE Trans. Wireless Communication*, vol. 4, no. 5, pp. 2441-2453, Sept. 2005.
- Oh, K. N. & Chin, Y. O. (1995). New blind equalization techniques based on constant modulus algorithm, in *Proc. Global Telecommunications Conference*, vol. 2, pp. 865-869, Nov. 1995.
- Ogawa, Y.; Fujishima, K. & Ohgane, T. (1999). Weighting factors in spatial domain path-diversity using an adaptive antenna," in *Proc. IEEE VTC'99*, vol. 3, pp. 2184-2188, May 1999.
- Sanada, Y. & Wang, Q. (1997). A co-channel interference cancellation technique using orthogonal convolutional codes on multipath Rayleigh fading channel, *IEEE Trans. Veh. Technol.*, vol. 46, no. 1, pp. 114-128, Feb. 1997.
- Saunders, S. R. (1999). *Antenna and Propagation for Wireless Communication Systems*. Chichester, England: John Wiley & Sons, Ltd., 1999.
- Slock, D. T. M. (1994). Blind joint equalization of multiple synchronous mobile users using over sampling and/or multiple antennas, in *Proc. IEEE Asilomar Conference on Signals, Systems and Computers*, vol. 2, pp. 1154-1158, 1994.
- Stott, J. H. (2000). The how and why of COFDM, tutorial COFDM, BBC Research and Development, http://www.ebu.ch/en/technical/trev/trev_278-stott.pdf.
- So, H. C.; Ching, P. C. & Chan, Y. T. (1994). New algorithm for explicit adaptation of time delay, *IEEE Trans. Signal Processing*, vol. 42, no. 7, pp. 1816-1820, July, 1994.
- Tanabe, Y. et al. (2000), An adaptive antenna for spatial-domain path-diversity using a super-resolution technique, in *Proc. IEEE VTC'00*, vol. 1, pp. 1-5, May 2000.
- Tanaka, T. (1994). A study on multipath propagation characteristics for RAKE receiving technique, in *Proc. 5th IEEE International Symposium on Personal, Indoor and Mobile Radio Communication*, vol. 2, pp. 711- 714, Sept. 1994.
- Valimaki, V. & Laakso, T. I. (2000). Principles of fractional delay filters," in *Proc. IEEE ICASS*, vol. 6, pp. 3870-3873, June 2000.
- Widrow, B.; Mantey, P. E.; Griffiths, L. J. & Goode, B. B. (1967). Adaptive antenna systems," *Proc. IEEE*, vol. 55, no. 12, pp. 2143-2159, Dec. 1967.
- Youna, W. S. & Un, C. K. (1994). Robust adaptive beamforming based on the eigen-structure method, *IEEE Trans. Signal Processing*, vol. 42, no. 6, pp. 1543-1547, June 1994.
- Yuan, J.T. & Tsai, K.D. (2005). Analysis of the multimodulus blind equalization algorithm in QAM communication systems, *IEEE Transactions on Communications*, vol. 53, no. 9, pp. 1427-1431, 2005.